

AD A 036377

12  
B.C.

ARPA ORDER NO.: 189-1  
7G10 Tactical Technology

R-1966-ARPA  
February 1977

# The Buoyancy and Variable Viscosity Effects on a Water Laminar Boundary Layer along a Heated Longitudinal Horizontal Cylinder

Lun-Shin Yao, Ivan Catton

DDC  
DEFENSE  
MAR 4 1977  
QUESTIONS

A Report prepared for  
DEFENSE ADVANCED RESEARCH PROJECTS AGENCY

DISTRIBUTION STATEMENT A  
Approved for public release  
Distribution Unlimited

**Rand**  
SANTA MONICA, CA. 90406

**The research described in this report was sponsored by the Defense Advanced Research Projects Agency under Contract No. DAHC15-73-C-0181.**

**Reports of The Rand Corporation do not necessarily reflect the opinions or policies of the sponsors of Rand research.**

R-1966-ARPA  
February 1977

# The Buoyancy and Variable Viscosity Effects on a Water Laminar Boundary Layer along a Heated Longitudinal Horizontal Cylinder

Lun-Shin Yao, Ivan Catton

A Report prepared for  
DEFENSE ADVANCED RESEARCH PROJECTS AGENCY

ACCESSION FOR	White Section	<input checked="" type="checkbox"/>	<input type="checkbox"/>	<input type="checkbox"/>
HQS	Blue Section			
DOC	White Section			
UNCLASSIFIED				
JUSTIFICATION				
BY	DISTRIBUTION/AVAILABILITY CODES			
	DIST.	AVAIL.	and/or SPECIAL	
			A	



UNCLASSIFIED

SECURITY CLASSIFICATION OF THIS PAGE (When Data Entered)

REPORT DOCUMENTATION PAGE		READ INSTRUCTIONS BEFORE COMPLETING FORM
1. REPORT NUMBER (14) R-1966-ARPA ✓	2. GOVT ACCESSION NO.	3. RECIPIENT'S CATALOG NUMBER
4. TITLE (and Subtitle) (6) The Buoyancy and Variable Viscosity Effects on a Water Laminar Boundary Layer Along a Heated Longitudinal Horizontal Cylinder,		5. TYPE OF REPORT & PERIOD COVERED Interim
7. AUTHOR(s) (10) Lun-Shin/Yao and Ivan/Catton		6. PERFORMING ORG. REPORT NUMBER
9. PERFORMING ORGANIZATION NAME AND ADDRESS The Rand Corporation 1700 Main Street Santa Monica, Ca. 90406		8. CONTRACT OR GRANT NUMBER(s) (15) DAHC15-73-C-0181 WARPA Order-189
11. CONTROLLING OFFICE NAME AND ADDRESS Defense Advanced Research Projects Agency, Department of Defense Arlington, Va. 22209		10. PROGRAM ELEMENT, PROJECT, TASK AREA & WORK UNIT NUMBERS
14. MONITORING AGENCY NAME & ADDRESS (if different from Controlling Office)		12. REPORT DATE (11) February 1977
		13. NUMBER OF PAGES (12) 33 p. 23
		15. SECURITY CLASS. (of this report) UNCLASSIFIED
16. DISTRIBUTION STATEMENT (of this Report)  Approved for Public Release; Distribution Unlimited		15a. DECLASSIFICATION/DOWNGRADING SCHEDULE
17. DISTRIBUTION STATEMENT (of the abstract entered in Block 20, if different from Report)  No restrictions		
18. SUPPLEMENTARY NOTES		
19. KEY WORDS (Continue on reverse side if necessary and identify by block number) Laminar Boundary Layer      Hydrodynamics Buoyancy      Fluid Mechanics Viscosity      Underwater Vehicles Water      Submarines		
20. ABSTRACT (Continue on reverse side if necessary and identify by block number)  see reverse side		

DD FORM 1 JAN 73 1473

EDITION OF 1 NOV 65 IS OBSOLETE

UNCLASSIFIED

SECURITY CLASSIFICATION OF THIS PAGE (When Data Entered)

296600

D D C  
 REPRODUCED  
 MAR 4 1977  
 REGISTERED

Small cross flow is induced in an otherwise axially symmetric laminar boundary layer when a uniform horizontal stream flows along the inner or outer surface of a heated horizontal cylinder. The magnitude of this cross flow depends on the ratio of the Grashof number to the square of the Reynolds number, based on the radius of the cylinder, and in its early stages grows linearly in the downstream direction. The report shows that the variable-viscosity effect can increase the velocity gradient and, hence, stabilize the laminar boundary layer; the cross-flow effect will decrease the velocity gradient and destabilize the laminar boundary layer over the upper half of the cylinder (or the pipe flow). Also, the boundary beyond which the cross-flow effect can overwhelm the variable-viscosity effect has been determined. (Author)

## PREFACE

Under the sponsorship of the Tactical Technology Office of the Defense Advanced Research Projects Agency, The Rand Corporation has been engaged in analysis for and development of hydrodynamic design criteria employing various concepts of boundary-layer control, including shaping, suction, and heating.

Stabilization of the laminar boundary layer over a horizontal axisymmetric body by heating may be upset by the buoyancy force induced by temperature differences. Using analytical methods, this report considers the combined effects of variable viscosity and buoyancy force over a heated cylinder, as a preliminary step toward defining a region where heating is a favorable method of stabilizing the boundary layer.

This report should be useful to hydrodynamicists, to designers of submersibles, and to others interested in applying fluid mechanics to the prediction and improvement of the performance of underwater vehicles.

Other, related Rand publications include:

R-1752-ARPA/ONR, *Low-Speed Boundary-Layer Transition Workshop*, William S. King, June 1975.

R-1789-ARPA, *Controlling the Separation of Laminar Boundary Layers in Water: Heating and Suction*, J. Aroesty and S. A. Berger, September 1975.

R-1863-ARPA, *The Effects of Wall Temperature and Suction on Laminar Boundary-Layer Stability*, William S. King, April 1976.

R-1866-ARPA, *Hydrodynamic Considerations in the Design of Small Submersible Vehicles (U)*, C. Gazley, Jr., J. Aroesty, W. S. King, and E. R. Van Driest, April 1976 (Confidential).

R-1898-ARPA, "*e*<sup>9</sup>" *Stability Theory and Boundary-Layer Transition*, S. A. Berger and J. Aroesty, in process.

R-1907-ARPA, *Buoyancy Cross-Flow Effects on the Boundary Layer of a Heated Horizontal Cylinder*, L. S. Yao and Ivan Catton, April 1976.

Lun-Shin Yao is a member of Rand's research staff; Ivan Catton is an Associate Professor of Engineering at the University of California, Los Angeles, and a consultant to The Rand Corporation.

## SUMMARY

The stabilization of laminar boundary layers under realistic circumstances requires attention to all those effects that could tilt the balance towards increased growth of disturbances. One such effect, occurring in heated boundary layers in water, is due to buoyancy-induced cross flow. A small cross flow is induced in an otherwise axially symmetric laminar boundary layer when a uniform horizontal stream flows along the inner or outer surface of a heated horizontal cylinder. The magnitude of this cross flow depends on the ratio of the Grashof number to the square of the Reynolds number, based on the radius of the cylinder, and in its early stages grows linearly in the downstream direction. The governing parameter,  $\epsilon = Gr/Re^2$ , is independent of viscosity and can be interpreted intuitively as the ratio of the heating-associated buoyancy force to the inertial force of the basic flow.

Earlier analysis, performed for a constant property flow, indicated that the cross flow could reduce heat transfer and shear stress over the upper half of the cylinder (or the pipe), while increasing it over the bottom half. More significantly, the cross-flow profiles were notoriously unstable, and their impact on hydrodynamic stability could be important, depending on the magnitude of  $\epsilon$ .

The present work extends the analysis in our earlier study to include the viscosity variation appropriate to water in the temperature range 40°F (4°C) to 100°F (37.8°C). The earliest effects of cross flow are studied and characterized by an expansion procedure in which the basic axially symmetric flow determines the leading term, the first corrections to axial velocity and temperature profiles are proportional to  $\epsilon(x/a)^2 \cos \phi$ , and the cross-flow component is proportional to  $\epsilon(x/a) \sin \phi$ .

The use of this expansion procedure bypasses the need for numerical calculation of three-dimensional boundary layers, provides solutions which are valid for realistic ranges of the parameters, and, because of their *explicit* dependence on the cross-flow parameter,  $\epsilon$ ,

can be later studied systematically for the effect on cross-flow stability of increasing the magnitude of  $\epsilon$ . However, the cross-flow effect on the flow transition can be qualitatively assessed by the variation of the velocity gradient on the wall. It has been demonstrated by Wazzan and Gazley\* (see Fig. 7) that the critical Reynolds number can be correlated approximately with the velocity gradient on the wall. The numerical results show that the variable-viscosity effect can increase the velocity gradient and, hence, stabilize the laminar boundary layer; the cross-flow effect will decrease the velocity gradient and destabilize the laminar boundary layer over the upper half of the cylinder (or the pipe flow). Also, the boundary beyond which the cross-flow effect can overwhelm the variable-viscosity effect has been determined.

The ratio of the maximum cross-flow velocity to the free-stream velocity,  $u_\infty$ , is about  $3 \times 10^{-3} (\Delta T / u_\infty^2) \cdot \bar{x}$ , where  $\Delta T$  is in  $^\circ\text{F}$ ,  $u_\infty$  is in ft/sec, and  $\bar{x}$  is in ft.

The analysis, which may easily be extended to larger values of  $\epsilon(\bar{x}/a)^2$ , is appropriate for estimating cross-flow effects for either external or internal flows and will be reported when it is finished. It is thus valid for describing the early stages of buoyancy-induced cross flow within a heated tube, where experiments are being conducted to verify the theoretical results.

---

\* A. R. Wazzan and C. Gazley, Jr., "A Parametric Study of Boundary-Layer Stability and Transition for Falkner-Skan Wedge Flows," presentation at *Low-Speed Boundary-Layer Transition Workshop: II*, held at The Rand Corporation, Santa Monica, California, September 13-15, 1976.



CONTENTS

PREFACE .....	iii
SUMMARY .....	v
FIGURES .....	ix
SYMBOLS .....	xi
Section	
I. INTRODUCTION .....	1
II. ANALYSIS .....	3
III. NUMERICAL RESULTS .....	11
IV. BUOYANCY VERSUS VARIABLE VISCOSITY .....	16
REFERENCES .....	23

FIGURES

1. Physical Model and Coordinates .....	3
2. Stream Function and Velocity Profiles Without Cross Flow .....	13
3. $F_1$ and $F'_1$ Functions .....	14
4. $F_2$ and $F'_2$ Functions .....	14
5. Temperature Distribution .....	15
6. Critical Reynolds Number Versus Wall Velocity Gradient .....	18
7. Boundary Where the Variable-Viscosity Effect Balances the Cross-Flow Effect .....	21

SYMBOLS

- $a$  = radius of the cylinder  
 $b, c$  = constants, Eq. (5)  
 $f$  = nondimensional stream function, Eqs. (9), (10), and (11)  
 $F$  = similarity nondimensional stream function, Eqs. (14) and (15)  
 $g$  = similarity nondimensional temperature, Eqs. (10) and (11)  
 $\bar{g}$  = gravitational acceleration, Eq. (2) =  $32.2 \text{ ft/sec}^2$   
 $G$  = similarity nondimensional temperature independent of  $\phi$ , Eqs. (14) and (15)  
 $Gr$  = Grashof number, Eq. (2)  
 $n$  = index, Eq. (17)  
 $N, N_0, N_1$  = viscosity ratios, Eqs. (2) and (6)  
 $Nu$  = Nusselt number, Eq. (21)  
 $Pr$  = Prandtl number, Eq. (2)  
 $r$  = nondimensional coordinate normal to the wall  
 $\bar{r}$  = radial coordinate  
 $Re$  = Reynolds number, Eq. (2)  
 $T$  = temperature  
 $u$  = axial velocity  
 $v$  = circumferential velocity  
 $w$  = radial velocity  
 $x$  = axial coordinate  
 $\alpha$  = coefficient for variable viscosity  
 $\beta$  = thermal expansion coefficient =  $0.8 \times 10^{-4} [^{\circ}\text{F}]^{-1}$   
 $\gamma$  = thermal diffusivity  
 $\epsilon = Gr/Re^2$ , Eq. (2)  
 $\eta = r/\sqrt{2x}$ , Blasius similarity variable, Eq. (9)  
 $\theta$  = nondimensional temperature, Eq. (2)  
 $\nu$  = kinematic viscosity  
 $\phi$  = circumferential coordinate  
 $\tau_{rx}$  = x-directional shear stress  
 $\tau_{r\phi}$  = circumferential shear stress

Subscripts

0 = zeroth-order solution  
00 = zeroth order of zeroth-order solution  
01 = first order of zeroth-order solution  
1 = first-order solution  
10 = zeroth order of first-order solution  
11 = first order of first-order solution  
2 = first order cross-flow solution  
w = surface  
 $\infty$  = free stream  
fc = forced convection

Superscripts

- = dimensional quantities  
' = derivative with respect to  $\eta$   
x = local quantities at location x

## I. INTRODUCTION

Laminar flow control, as the means to achieve low-drag performance, requires the careful manipulation of boundary-layer velocity profiles. Body shaping, pressure gradient, and suction are classic methods for such boundary-layer control.<sup>(1)</sup> For submersible applications the temperature-dependent viscosity of water provides the mechanism by which appropriate velocity profiles can be maintained by wall heating. These velocity profiles, as in the other methods, inhibit the amplification of two-dimensional Tollmein-Schlichting instability waves and thus retard boundary-layer transition until body shape and adverse pressure gradient force the separation of the laminar boundary layer. Suction and heating have similar effects on boundary-layer stability and transition, but the theoretical potential of suction for even further drag reduction by delaying laminar separation is greater.<sup>(2)</sup>

Historically, each method of boundary-layer control has had limitations, corresponding to the growth of disturbances associated with free-stream turbulence, surface roughness or waviness, noise, loss of suction effectiveness, or three-dimensionality. Surface heating shares these possible limits on performance and has some limits which are unique to it alone.

Temperature gradients in the boundary layer of a heated horizontal body result in buoyancy forces that induce small, steady, cross-flow velocities. These in turn could distort the basic laminar axisymmetric velocity profiles into three-dimensional ones, which are considerably less stable. Yao and Catton<sup>(3)</sup> earlier examined the development of this steady, slightly three-dimensional laminar boundary layer on a heated longitudinal horizontal cylinder for the case of constant fluid properties. Their results indicate that the cross flow can enhance the heat transfer and stabilize the boundary layer over the lower half of the cylinder, but it degrades heat transfer and destabilizes the flow over the upper half of the cylinder. Since the boundary layer is very thin compared with the curvature of the cylinder, the transverse curvature effect can be neglected. Also, the results can be applied to the entrance flow in a circular pipe.

The present paper extends that work to the realistic case of water, including the variable viscosity effect. Similarly, the results can be applied to the pipe flow near the entrance. In this way the domain where cross-flow effects may counterbalance the stabilizing variable viscosity effect may be established later by a more detailed three-dimensional stability analysis.

The physical model chosen is a semi-infinite cylinder of radius  $a$  (or in a horizontal pipe with radius  $a$ ), which is aligned with its axis parallel to a uniform flow and normal to the direction of gravity. The uniform flow is assumed to have a velocity  $u_\infty$  and temperature  $T_\infty$ . The surface of the cylinder is heated to a constant temperature  $T_w$  ( $T_w > T_\infty$ ). For water flow in the range of 40°F (4.4°C) and 100°F (37.8°C), the principal departure from constant property flow is due to viscosity variation. The thermal conductivity and specific heat do not vary appreciably in this range, and the most important phenomena, because of the gradient of viscosity, are quite well represented by the model in which  $k$  and  $c_p$  are constant, and the variation of viscosity with temperature is preserved. Since the density variation is small, the Boussinesq approximation is adopted, which treats the density as a constant in the equations of motion except for the buoyancy force term. The buoyancy cross flow is small in the leading-edge region of the cylinder and can be treated as a second-order effect. Further downstream, a distance of order  $a \cdot \text{Re}/\text{Gr}^{1/2}$ , the initially small buoyancy cross flow becomes one of the dominant velocity components and can no longer be treated as a second-order effect. The present analysis is valid under most practical circumstances, particularly when realistic magnitudes of  $1/\sqrt{\epsilon} = \text{Re}/\text{Gr}^{1/2} \equiv u_\infty/\sqrt{\beta g \Delta T a}$  are considered. For example, the analysis should provide an accurate approximation to the cross flow in the region  $0 < \bar{x} < a/\sqrt{\epsilon} = (u_\infty/\sqrt{\beta g \Delta T} \cdot \sqrt{a})$ , where  $\bar{x}$  is in ft,  $u_\infty$  is in ft/sec,  $\Delta T$  is in deg F, and  $a$  is in ft.

The ratio of the cross-flow component to the free-stream velocity is  $\beta g \Delta T \bar{x} / u_\infty^2 \cos \phi$ , or  $3 \times 10^{-3} (\Delta T / u_\infty^2) \times \bar{x} \cos \phi$ , in the same units.

## II. ANALYSIS

The governing equations of the flow with fluid of variable viscosity on a heated, longitudinal, horizontal cylinder are the Boussinesq boundary-layer equations. In cylindrical coordinates, as shown in Fig. 1, they are

$$\frac{\partial \bar{u}}{\partial \bar{x}} + \frac{1}{\bar{r}} \frac{\partial (\bar{r} \bar{w})}{\partial \bar{r}} + \frac{1}{\bar{r}} \frac{\partial \bar{v}}{\partial \bar{\phi}} = 0 \quad (1a)$$

$$\bar{u} \frac{\partial \bar{u}}{\partial \bar{x}} + \frac{\bar{v}}{\bar{r}} \frac{\partial \bar{u}}{\partial \bar{\phi}} + \bar{w} \frac{\partial \bar{u}}{\partial \bar{r}} = \frac{-1}{\rho_{\infty}} \frac{\partial \bar{p}}{\partial \bar{x}} + \frac{\partial}{\partial \bar{r}} \left( \nu \frac{\partial \bar{u}}{\partial \bar{r}} \right) \quad (1b)$$

$$\bar{u} \frac{\partial \bar{w}}{\partial \bar{x}} + \frac{\bar{v}}{\bar{r}} \frac{\partial \bar{w}}{\partial \bar{\phi}} + \bar{w} \frac{\partial \bar{w}}{\partial \bar{r}} = (\bar{g} \beta \Delta T) \cos \phi - \frac{1}{\rho_{\infty}} \frac{\partial \bar{p}}{\partial \bar{r}} + \frac{\partial}{\partial \bar{r}} \left( \nu \frac{\partial \bar{w}}{\partial \bar{r}} \right) \quad (1c)$$

$$\bar{u} \frac{\partial \bar{v}}{\partial \bar{x}} + \frac{\bar{v}}{\bar{r}} \frac{\partial \bar{v}}{\partial \bar{\phi}} + \bar{w} \frac{\partial \bar{v}}{\partial \bar{r}} = (\bar{g} \beta \Delta T) \sin \phi - \frac{1}{\bar{r} \rho_{\infty}} \frac{\partial \bar{p}}{\partial \bar{\phi}} + \frac{\partial}{\partial \bar{r}} \left( \nu \frac{\partial \bar{v}}{\partial \bar{r}} \right) \quad (1d)$$

$$\bar{u} \frac{\partial T}{\partial \bar{x}} + \frac{\bar{v}}{\bar{r}} \frac{\partial T}{\partial \bar{\phi}} + \bar{w} \frac{\partial T}{\partial \bar{r}} = \alpha \frac{\partial^2 T}{\partial \bar{r}^2} \quad (1e)$$

Equations (1) are also valid for the entrance flow in a heated pipe.

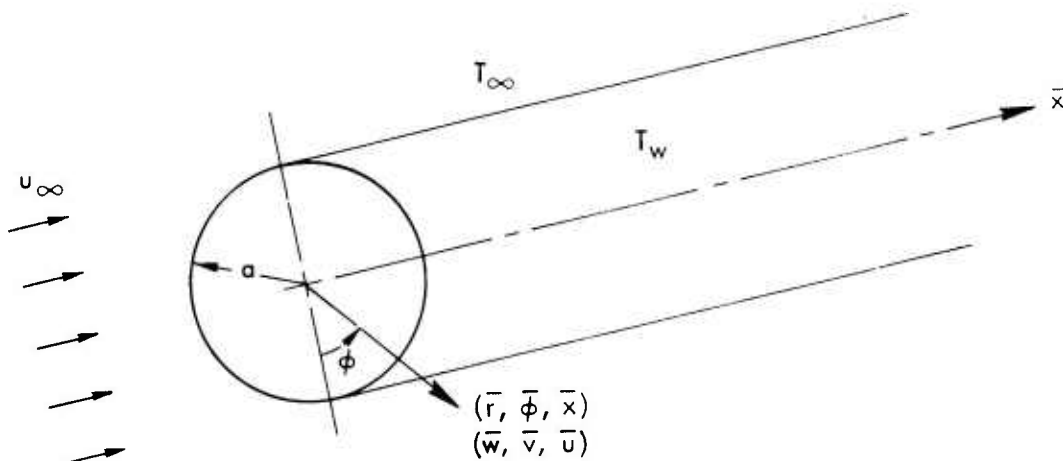


Fig. 1—Physical model and coordinates

The dimensionless variables that are introduced to nondimensionalize Eqs. (1) are

$$\begin{aligned}
 u &= \frac{\bar{u}}{u_\infty}, \quad v = \frac{\bar{v}}{u_\infty}, \quad w = \frac{\bar{w}\sqrt{Re}}{u_\infty} && \text{(the velocities)} \\
 \theta &= \frac{T - T_\infty}{T_w - T_\infty} && \text{(the temperature)} \\
 x &= \frac{\bar{x}}{a}, \quad r = \frac{(\bar{r} - a)\sqrt{Re}}{a} && \text{(the coordinates)} \\
 Re &= \frac{u_\infty a}{\nu} && \text{(the Reynolds number)} \\
 Gr &= \frac{\beta g a^3 (T_w - T_\infty)}{\nu^2} && \text{(the Grashof number)} \\
 Pr &= \frac{\nu_\infty}{\gamma} && \text{(the Prandtl number)} \\
 \epsilon &= \frac{Gr}{Re^2} \\
 N &= \frac{\mu}{\mu_\infty}
 \end{aligned} \tag{2}$$

The radius of the cylinder,  $a$ , has been selected as the longitudinal characteristic length in order to study the detailed development of the mechanism of the induced cross flow caused by heating along the upstream part of the horizontal cylinder. The coordinate normal to the wall has been stretched to reflect the fact that the thickness of the boundary layer in the region of  $\bar{x} \sim 0(a)$  is inversely proportional to the square root of the Reynolds number.

We note that the quantity  $\epsilon$  can be expressed simply as  $\beta g (T_w - T_\infty) a / u_\infty^2$  and can be interpreted as the ratio of the potential energy increment



to the kinetic energy of the flow. For the flow close to the leading edge of the cylinder (or close to the entrance of a pipe), the magnitude of  $\epsilon$  determines the importance of the thermally driven cross flow. As we move further downstream, the governing parameter will be the Grashof number instead of  $\epsilon$ . There the cross flow can be neglected only when the Grashof number is small. For our case, where the Grashof number is not small but  $Gr/Re^2$  is small, the cross-flow effect can be treated as a secondary effect in the region near the leading edge of the cylinder (or near the entrance of the pipe). The magnitude of the cross flow develops and eventually becomes one of the dominant phenomena which can trigger the flow transition and the flow separation further downstream. It is worth noting that the value of  $\epsilon$  also determines the size of the early region where the cross flow is a second-order effect when  $Gr > 1$  and  $Gr/Re^2 < 1$ . In terms of the dimensionless parameters in Eq. (2), Eqs. (1) become

$$\frac{\partial u}{\partial x} + \frac{\partial w}{\partial r} + \frac{\partial v}{\partial \phi} = 0 \quad (3a)$$

$$u \frac{\partial u}{\partial x} + v \frac{\partial u}{\partial \phi} + w \frac{\partial u}{\partial r} = - \frac{\partial p}{\partial x} + \frac{\partial}{\partial r} \left( N \frac{\partial u}{\partial r} \right) \quad (3b)$$

$$\frac{\partial p}{\partial r} = \frac{\epsilon}{\sqrt{Re}} \cdot \theta \cdot \cos \phi \quad (3c)$$

$$u \frac{\partial v}{\partial x} + v \frac{\partial v}{\partial \phi} + w \frac{\partial v}{\partial r} = \epsilon \cdot \sin \phi \cdot \theta - \frac{\partial p}{\partial \phi} + \frac{\partial}{\partial r} \left( N \frac{\partial v}{\partial r} \right) \quad (3d)$$

$$u \frac{\partial \theta}{\partial x} + v \frac{\partial \theta}{\partial \phi} + w \frac{\partial \theta}{\partial r} = \frac{1}{Pr} \frac{\partial^2 \theta}{\partial r^2} \quad (3e)$$

after neglecting smaller-order terms. The terms that represent the transverse curvature effect have been neglected simply because the boundary layer is thin compared with the radius of the cylinder when the Reynolds number is not small. Equation (3c) indicates that the pressure gradient normal to the wall is negligible to the lowest order,

and the pressure gradients parallel to the wall can be evaluated from the inviscid solution at the edge of the boundary layer. For a uniform free stream, these pressure gradients vanish.

It is necessary to specify the viscosity ratio,  $N$ , before the solutions of Eqs. (3) can be presented. It has been shown by Gazley\* that a good approximation for the kinematic viscosity of water in the range of temperature between 40°F (4.4°C) and 100°F (37.8°C) is

$$\nu = \frac{10^{-5}}{-0.0807 + 0.0126T} \quad (4)$$

where  $T$  is in °F and  $\nu$  is in ft<sup>2</sup>/sec. This suggests a viscosity-temperature model of the form

$$\mu = \frac{1}{b + cT} \quad (5)$$

For such a model,

$$\frac{1}{N} = \frac{\mu_{\infty}}{\mu} = 1 + \alpha \Delta T \cdot \theta \quad (6)$$

where  $\Delta T = T_w - T_{\infty}$ , and  $\alpha = c/(b + cT_{\infty})$ . For water in the temperature range between 40°F (4.4°C) and 100°F (37.8°C),  $\alpha \approx 0.0151$  (°F)<sup>-1</sup>. It has also been shown by Gazley that the Prandtl number of water in the range of temperature 40°F (4.4°C) and 100°F (37.8°C) can be approximated by

$$Pr = \frac{455}{T_{\infty}} \quad (7)$$

where  $T_{\infty}$  is in °F. The illustrative calculations described below were performed using a value of  $Pr = 8$ .

---

\*Personal communication from Carl Gazley, Jr., The Rand Corporation, 1976.

The solution of Eqs. (3) with the viscosity-temperature model, Eq. (6), can be expanded into a series in  $\epsilon$ , if  $\epsilon$  is small, so that

$$u = u_0 + \epsilon u_1 + \dots \quad (8a)$$

$$v = \epsilon v_1 + \dots \quad (8b)$$

$$w = w_0 + \epsilon w_1 + \dots \quad (8c)$$

$$\theta = \theta_0 + \epsilon \theta_1 + \dots \quad (8d)$$

$$N = N_0 + \epsilon N_1 + \dots \quad (8e)$$

where

$$N_0 = \frac{1}{1 + \alpha \Delta T \theta_0} \quad (8f)$$

$$N_1 = \frac{-\alpha \Delta T}{(1 + \alpha \Delta T \theta_0)^2} \cdot \theta_1 = A(\theta_0) \cdot \theta_1 \quad (8g)$$

Substitution of the expansion given by Eqs. (8) into Eqs. (3), and the collection of terms of equal order will result in the perturbation equations. The perturbation equations of lowest order are

$$(\epsilon^0): (N_0 f_0'')' + f_0 f_0'' = 0 \quad (9a)$$

$$\theta_0'' + \text{Pr} f_0 \theta_0' = 0 \quad (9b)$$

where the prime denotes a derivative with respect to  $\eta$ , with  $\eta = r/\sqrt{2x}$  being the Blasius similarity variable. The stream function  $f_0$  is defined by

$$u_0 = f_0' \quad (9c)$$

$$w_0 = \frac{1}{\sqrt{2x}} (\eta f_0' - f_0) \quad (9d)$$

The second-order perturbation equations are

$$(\epsilon^1): (N_0 f_1'')' + f_0 f_1'' - 4f_0' f_1' + 5f_0'' f_1 + f_0'' \frac{\partial f_2}{\partial \phi} = (A \cdot g \cdot f_0'')' \quad (10a)$$

$$(N_0 f_2'')' + f_0 f_2'' - 2f_0' f_2' + \sin \phi \cdot \theta_0 = 0 \quad (10b)$$

$$\frac{1}{Pr} g'' + f_0 g' - 4f_0' g + 5\theta_0' f_1 + \theta_0' \frac{\partial f_2}{\partial \phi} = 0 \quad (10c)$$

The stream functions  $f_1$  and  $f_2$  and the temperature  $g$  are defined by

$$\left. \begin{aligned} u_1 &= (2x)^2 f_1'(\eta, \phi) \\ v_1 &= (2x) f_2'(\eta, \phi) \\ w_1 &= (2x)^{3/2} \left( \eta f_1' - 5f_1 - \frac{\partial f_2}{\partial \phi} \right) \\ \theta_1 &= (2x)^2 g(\eta, \phi) \end{aligned} \right\} \quad (11)$$

The boundary conditions associated with Eqs. (9) are

$$\left. \begin{aligned} f_0 &= f_0' = 0 \quad \text{and} \quad \theta_0 = 1 \quad \text{at} \quad \eta = 0 \\ f_0' &\rightarrow 1 \quad \text{and} \quad \theta_0 \rightarrow 0 \quad \text{as} \quad \eta \rightarrow \infty \end{aligned} \right\} \quad (12)$$

and the ones associated with Eqs. (10) are

$$\left. \begin{aligned} f_1' &= f_2' = f_1 = \frac{\partial f_2}{\partial \phi} = 0, \quad g = 0 \quad \text{at} \quad \eta = 0 \\ f_1' &= f_2' = 0, \quad g = 0 \quad \text{as} \quad \eta \rightarrow \infty \\ f_2' &= 0 \quad \text{at} \quad \phi = 0, \pi \end{aligned} \right\} \quad (13)$$

Equations (10) are separable in terms of  $\eta$  and  $\phi$  with dependent variables of the form

$$\left. \begin{aligned} f_1(\eta, \phi) &= F_1(\eta) \cos \phi \\ f_2(\eta, \phi) &= F_2(\eta) \sin \phi \\ g(\eta, \phi) &= G(\eta) \cos \phi \end{aligned} \right\} \quad (14)$$

Substituting Eqs. (14) into Eqs. (10) gives

$$(N_0 F_1'')' + f_0 F_1'' - 4f_0' F_1' - 5f_0'' F_1 + f_0'' F_2 = (A \cdot G \cdot f_0'')' \quad (15a)$$

$$(N_0 F_2'')' + f_0 F_2'' - 2f_0' F_2' = -\theta_0 \quad (15b)$$

$$\frac{1}{Pr} G'' + f_0 G' - 4f_0' G = -\theta_0' (5F_1 + F_2) \quad (15c)$$

The associated boundary conditions for Eqs. (10) are

$$\left. \begin{aligned} F_1(0) &= F_1'(0) = F_1'(\infty) = 0 \\ F_2(0) &= F_2'(0) = F_2'(\infty) = 0 \\ G(0) &= G(\infty) = 0 \end{aligned} \right\} \quad (16)$$

The solutions depend on temperature only through the factor  $\alpha \Delta T$  and are integrated numerically for  $\alpha \cdot \Delta T = 0, .5, 1.0$ . If  $T_\infty = 57^\circ F$ , this corresponds to  $\Delta T = 0, 33^\circ, 66^\circ$ .

The form of the solution suggests that a continuation of this expansion procedure along the lines

$$\left. \begin{aligned} u &= \sum_{n=0}^{\infty} u_n(\eta, \phi) (\epsilon x^2)^n \\ \theta &= \sum_{n=0}^{\infty} \theta_n(\eta, \phi) (\epsilon x^2)^n \\ v &= \epsilon x \sum_{n=0}^{\infty} v_n(\eta, \phi) (\epsilon x^2)^n \end{aligned} \right\} \quad (17)$$

would be the appropriate continuation scheme further downstream. Convergence of this expansion presumably requires that  $\epsilon x^2$  be less than unity, and the accuracy of the two-term expansion for  $u$  and  $\theta$  and the one-term expansion for  $v$  requires that  $\epsilon x^2$  be small.\*

---

\* Preliminary numerical computations at Rand of the three-dimensional momentum integral boundary-layer equation suggest that the solution given by Eq. (17) is valid for  $0 < \epsilon x^2 < .2$ . However, the limits of validity of the analysis and regions where the cross flow may balance or even dominate the variable-viscosity effect can be better determined after more computations of the downstream three-dimensional boundary-layer flow are completed.

### III. NUMERICAL RESULTS

The physical quantities of velocity and temperature can be expressed in terms of the functions defined in Eqs. (8), (9), and (11). They are

$$u = f'_0 + \varepsilon(2x)^2 F'_1 \cdot \cos \phi + \dots \quad (18a)$$

$$v = \varepsilon(2x) \cdot F'_2 \cdot \sin \phi + \dots \quad (18b)$$

$$w = \frac{1}{\sqrt{2x}} (\eta f'_0 - f_0) + \varepsilon(2x)^{3/2} (\eta F'_1 - 5F_1 - F_2) \cdot \cos \phi + \dots \quad (18c)$$

$$\theta = \theta_0 + \varepsilon(2x)^2 \cdot G \cdot \cos \phi + \dots \quad (18d)$$

The local shear stress at the cylinder can be computed from the axial and cross-flow velocity components:

$$\tau_{rx} = \mu \left( \frac{\partial u}{\partial r} \right)_{r=0} \quad \text{and} \quad \tau_{r\phi} = \mu \left( \frac{\partial v}{\partial r} \right)_{r=0}$$

Introducing the series expansion (18), this can be written as

$$\frac{\tau_{rx}}{(\tau_{rx})_{fc}} = 1 + \varepsilon(2x)^2 \frac{F''_1(0)}{f''_0(0)} \cdot \cos \phi + \dots \quad (19)$$

for the axial shear and

$$\tau_{r\phi} \sim \varepsilon \sqrt{2x} F''_2(0) \sin \phi \quad (20)$$

for the circumferential component, where  $fc$  denotes the value for forced convection with variable viscosity.

The local Nusselt number can be written as

$$\frac{Nu}{Nu_{fc}} = 1 + \epsilon(2x)^2 \cdot \frac{G'(0)}{\theta'_0(0)} \cdot \cos \phi + \dots \quad (21)$$

Table 1 shows the values of the quantities  $F_1''(0)/f_0''(0)$ ,  $G'(0)/\theta'_0(0)$ , and  $F_2''(0)$ . It is worth noting that the relative modifications of the axial stress and heat transfer caused by cross flow are both small (<9 percent) and insensitive to wall temperature in the range  $0 \leq \alpha \Delta T \leq 1$ , or up to  $\Delta T \sim 66^\circ\text{F}$ . The circumferential velocity gradient, on the other hand, shows a considerable variation with wall temperature, increasing 50 percent in the range between  $\alpha = 0$  and  $\alpha \Delta T = 1$ . Interestingly, the increase in the coefficient  $F_2''(0)$  is balanced by the decrease in the wall viscosity caused by heating, and the quantity  $\tau_{r\phi}$ , the product of the velocity gradient and the viscosity at the wall, actually decreases by 25 percent in the range between  $\alpha = 0$  and  $\alpha \Delta T = 1$ .

Table 1

ENHANCEMENT PARAMETERS FOR HEAT TRANSFER  
AND WALL SHEAR STRESS

	$G'(0)/\theta'_0(0)$	$F_1''(0)/f_0''(0)$	$F_2''(0)$
$\alpha = 0$	0.06981	0.04905	0.41499
$\alpha \Delta T = 0.5$	0.06559	0.04897	0.53625
$\alpha \Delta T = 1.0$	0.06296	0.04899	0.63888

From Figs. 2, 3, and 4 we observe that the reduction of water viscosity caused by heating modifies the axial flow: The axial flow is accelerated by the induced cross flow over the lower half of the cylinder ( $-\pi/2 < \phi < \pi/2$ ) and decelerated over the upper half ( $\pi/2 < \phi < 3\pi/2$ ). The cross flow is accelerated by buoyancy from the lower stagnation point ( $\phi = 0$ ) to its maximum value at  $\phi = \pi/2$  and then decelerated to its upper stagnation point ( $\phi = \pi$ ). The decrease



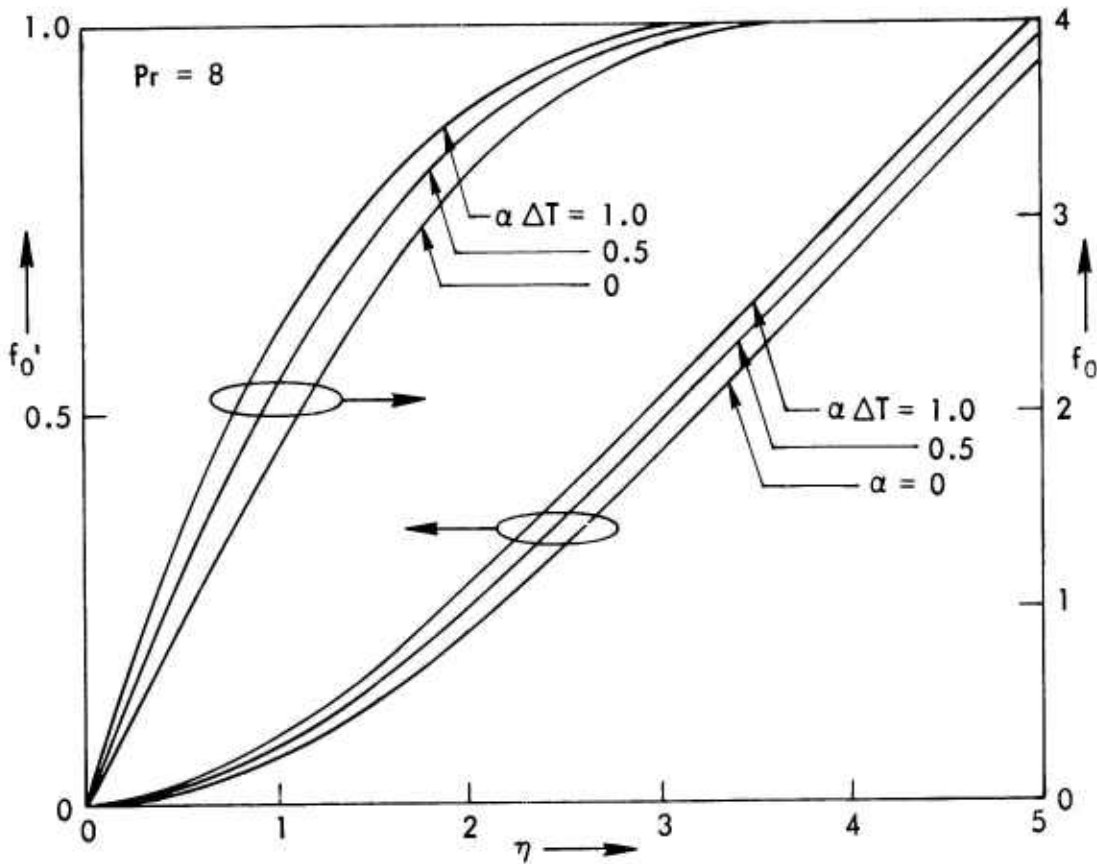


Fig. 2—Stream function and velocity profiles without cross flow

of viscosity by heating enhances the magnitude of the cross flow ( $F_2'$ ) and shifts the point of maximum velocity to the wall as shown in Fig. 4. Therefore, the cross-flow velocity gradient at the wall magnified appreciably by a slight variation of the fluid viscosity. The induced axial velocity  $F_1'$  becomes more full in the wall region, as wall temperature increases. The key differences between the cross-flow velocity  $F_2'$  and the co-induced axial velocity  $F_1'$  is that the maximum value of  $F_2'$  increases from 0.118 to 0.107 as  $\alpha \Delta T$  increases from 0 to 1, while the maximum value of  $F_1'$  decreases from .021 to .015 over the same range. Since the maximum value of  $F_1'$  is so small, this suggests that the effect of buoyancy on the boundary-layer displacement and momentum thicknesses,  $\delta^*$  and  $\theta$ , would be negligible in this region.

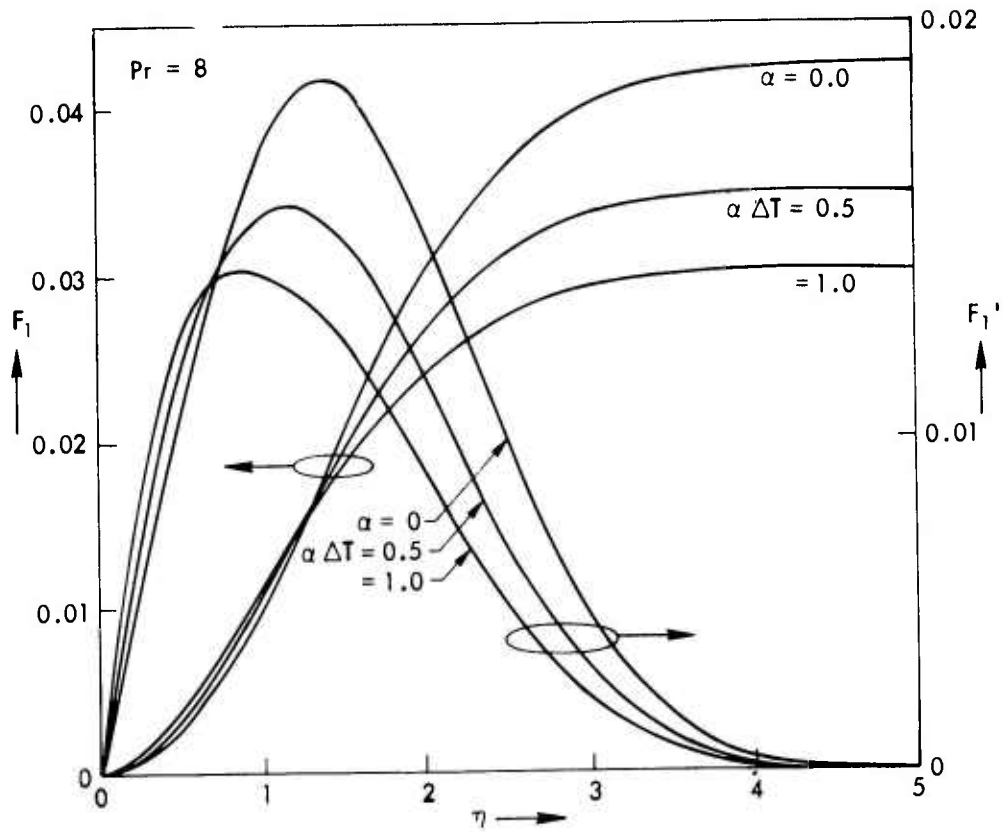


Fig. 3 —  $F_1$  and  $F_1'$  functions

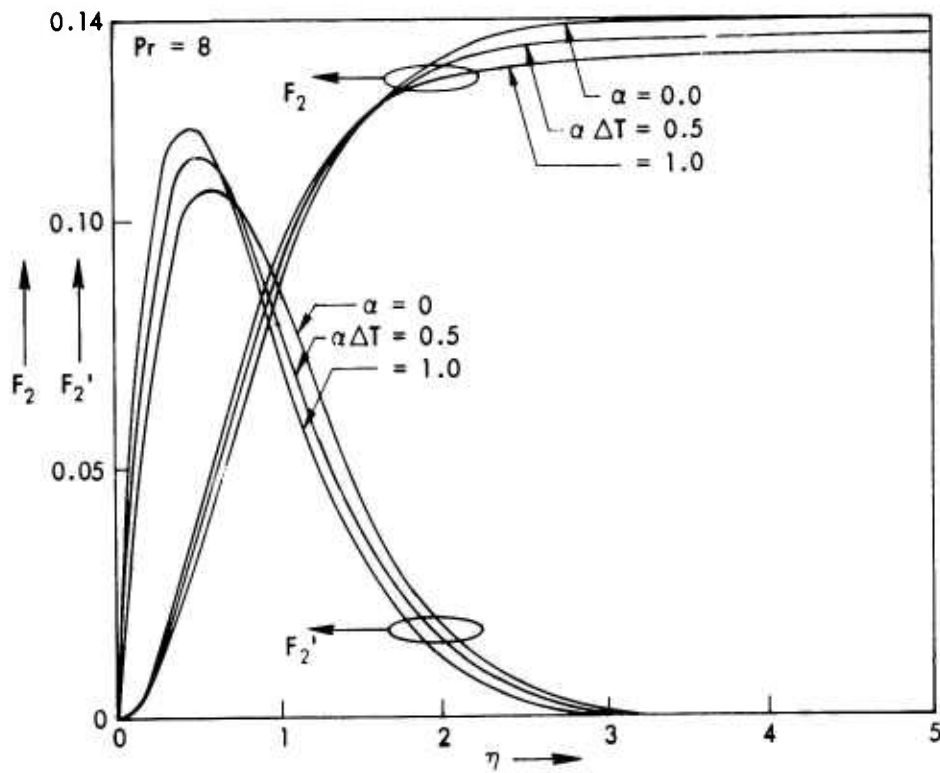


Fig. 4 —  $F_2$  and  $F_2'$  functions

From Fig. 5 it can be seen that the effect of heating on the buoyancy correction  $G$  is negligible in the region near the wall, but the maximum value of  $G$  decreases slightly as  $\alpha \Delta T$  increases. Since the maximum value of  $G$  is only .03, the cross-flow effect on the temperature field is negligible in this region. However, the primary distribution of the temperature gradient,  $\theta'_0$ , varies about 10 percent in the range between  $\alpha = 0$  and  $\alpha \Delta T = 1$ .

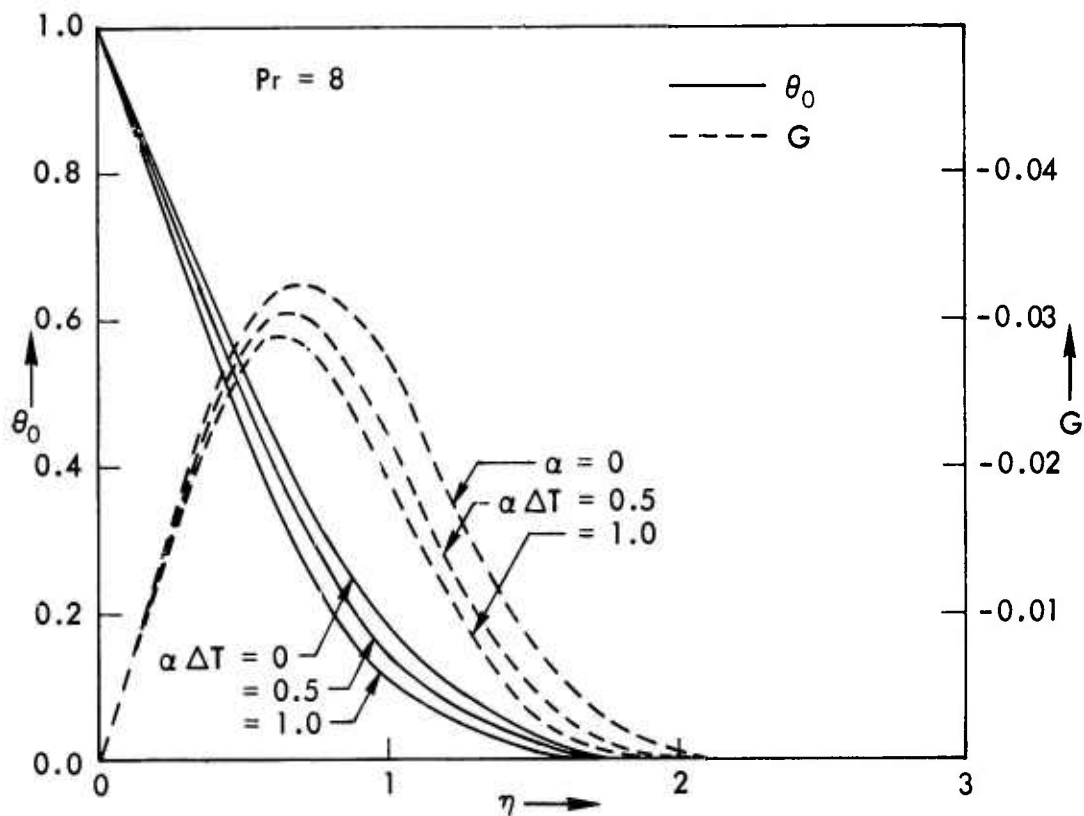


Fig. 5—Temperature distribution

#### IV. BUOYANCY VERSUS VARIABLE VISCOSITY

The primary importance of cross flow is the stability of the resulting three-dimensional boundary layer, and this will be considered in subsequent research. However, it is still of some interest to compare the magnitudes of the buoyancy effect with the variable viscosity effect, in order to further delineate the region where buoyancy effects on shear stress, heat transfer, and separation may safely be neglected.

While the solutions of Eqs. (9) and (15) correspond to the most general case of arbitrarily large viscosity variation, explicit estimates of the region where buoyancy effects on heat transfer and axial velocity profiles start to be important can be obtained by a further approximation.

If the viscosity variation is small, because of small values of  $\alpha \Delta T$ , the effect of variable viscosity can be separated out from the first-order Eqs. (9a) and (9b) by a linearization procedure. When  $\alpha = 0$ , the solution of Eq. (9a) corresponds to the Blasius solution. The expansion procedure becomes

$$\left. \begin{aligned} f_0 &= f_{00} + (\alpha \Delta T) \cdot f_{01} + \dots \\ \theta_0 &= \theta_{00} + (\alpha \Delta T) \cdot \theta_{01} + \dots \end{aligned} \right\} \quad (22)$$

Substitution of Eqs. (18) into Eqs. (9a) and (9b), or collecting terms of equal order, gives the equations of the zeroth order

$$f_{00}''' + f_{00} f_{00}'' = 0 \quad (23a)$$

$$\frac{1}{Pr} \theta_{00}'' + f_{00} \theta_{00}' = 0 \quad (23b)$$

and the equations of the first order

$$f_{01}''' + (f_{00}f_{01}'' + f_{00}''f_{01}) = (\theta_{00}f_{00}'')' \quad (24a)$$

$$\frac{1}{Pr} \theta_{01}'' + f_{00}\theta_{01}' + f_{01}\theta_{00}' = 0 \quad (24b)$$

The associated boundary conditions

$$\left. \begin{aligned} f_{00}(0) = f_{00}'(0) = 0, \quad f_{00}'(\infty) = 1 \\ \theta_{00}(0) = 1, \quad \theta_{00}(\infty) = 0 \\ f_{01}(0) = f_{01}'(0) = f_{01}'(\infty) = 0 \\ \theta_{01}(0) = \theta_{01}(\infty) = 0 \end{aligned} \right\} \quad (25)$$

The solution of Eq. (23a) is the Blasius solution; the solution of Eq. (23b) is the forced-convection energy equation. The functions  $f_{01}$  and  $\theta_{01}$  represent the effect of the variable viscosity on the forced convection. The numerical values of  $\theta_{01}$  and  $f_{01}$  can be obtained by integrating Eq. (24) numerically. Strictly speaking, the above approach is valid only for small values of  $\alpha \Delta T$ . However, comparison with the solution of Eq. (9) shows that this linearization is accurate in the range  $0 < \alpha \Delta T < 0.5$ .

The decrease of the water viscosity caused by heating will increase the axial velocity gradient on the wall and consequently will tend to stabilize the boundary layer.<sup>(2,3)</sup> For a horizontal cylinder, the cross flow will be induced by wall heating as a by-product, which will decrease the axial velocity gradient on the wall. In general, the stability of a boundary layer is related to this velocity gradient on the wall as has been demonstrated by Wazzan and Gazley, Jr.<sup>(4)</sup> and shown in Fig. 6. Based on this observation, the cross flow seems to introduce a destabilizing effect on the boundary layer. Also, the inflection point of the cross-flow velocity profile could be unstable. The conditions leading to flow transition can only be defined by extensive stability analysis. Before we can exercise such a complicated

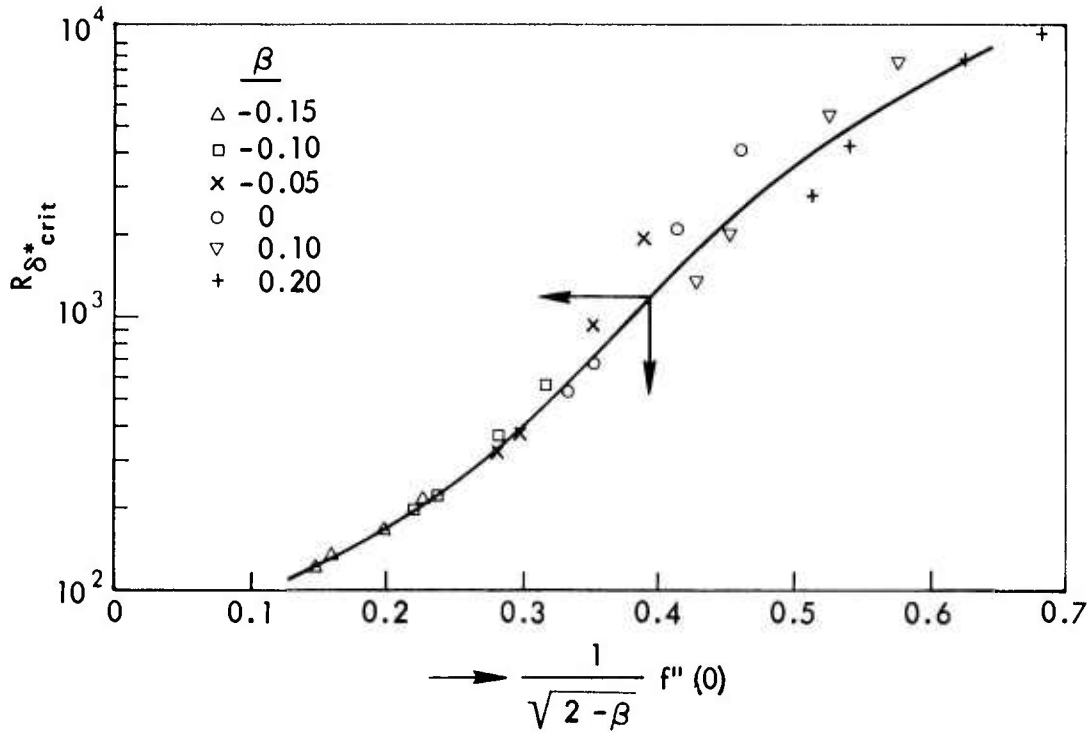


Fig. 6—Critical Reynolds number versus wall velocity gradient  
( $\beta$  is related to the wedge angle)

three-dimensional stability analysis, we will apply a simple criterion, the variation of axial velocity gradient on the wall, to study the tendency of stabilizing or destabilizing the boundary layer by heating.

The purpose of the study in this section is to provide some insight into the balancing effects of variable viscosity and cross flow. Thus the discussion is limited to the case of small values of  $\alpha \Delta T$  in order to supply a simple criterion to define a region and its functional dependence that heating is a practical way to stabilize the boundary layer.

The double expansion of velocity and temperature in terms of  $\epsilon$  and  $\alpha \Delta T$  can be written:

$$u = f'_{00} + (\alpha \Delta T) f'_{01} + \varepsilon (2x)^2 [F'_{10} + (\alpha \Delta T) F'_{11}] \cos \phi + \dots \quad (26a)$$

$$\theta = \theta_{00} + (\alpha \Delta T) \theta_{01} + \varepsilon (2x)^2 [G_0 + (\alpha \Delta T) G_1] \cos \phi + \dots \quad (26b)$$

where

$$\left. \begin{aligned} F_1 &= F_{10} + (\alpha \Delta T) F_{11} + \dots \\ G &= G_0 + (\alpha \Delta T) G_1 + \dots \end{aligned} \right\} \quad (27)$$

and  $F_{10}$  and  $G_0$  are the first-order-solution, cross-flow-induced quantities, with a constant property assumption.

The local shear stress, Eq. (19), can be further expanded. It becomes

$$\frac{\tau_{rx}}{(\tau_{rx})_{fc}} = 1 + (\alpha \Delta T) \frac{f''_{01}(0)}{f''_{00}(0)} + \varepsilon (2x)^2 \frac{F''_{10}(0)}{f''_{00}(0)} \cdot \cos \phi + \dots \quad (28)$$

where  $fc$  denotes the case of forced convection with constant viscosity. Since the wall viscosities are the same, Eq. (28) can be viewed as the ratio of the velocity gradients at the wall. Values of  $f''_{01}(0)/f''_{00}(0)$  and  $F''_{10}(0)/f''_{00}(0)$  are given in Table 2, and  $f''_{01}(0)/f''_{00}(0)$  is about twenty times bigger than  $F''_{10}(0)/f''_{00}(0)$ . This indicates that the variable-viscosity effect overwhelms the cross-flow effect over the most forward part of the cylinder. However, the magnitude of the cross-flow effect

Table 2

RATIOS OF HEAT FLUX AND SHEAR STRESS

$f''_{01}(0)/f''_{00}(0)$	$F''_{10}(0)/f''_{00}(0)$	$\theta'_{01}(0)/\theta'_{00}(0)$	$G'_0(0)/\theta'_{00}(0)$
0.89169	0.04905	0.17791	0.06981

increases as  $\sim x^2$  downstream. The variable-viscosity effect is eventually balanced by the cross-flow effect far away from the leading edge. Equation (28) clearly points out the location where the effect of stabilizing the boundary layer by heating will be balanced by the destabilizing cross-flow effect over the upper half of the cylinder ( $\pi/2 < \phi < 3\pi/2$ ). This location can be found from Eq. (28) by equating the second and the third terms on the right-hand side, which yields

$$x = \frac{1}{2} \left[ \frac{(\alpha \Delta T)}{\epsilon} \frac{f''_{01}(0)}{F''_{10}(0)} \right]^{1/2} \cdot \frac{1}{\sqrt{|\cos \phi|}} \quad (29)$$

Equation (29) is plotted in Fig. 7, which shows that the region of stabilizing the boundary layer by heating shrinks as  $x$  increases. It should be noted that the expansions (23) are valid only up to  $x \sim O(1/\sqrt{\epsilon})$  and then the originally small cross flow becomes one of the dominant velocity components beyond  $x \sim O(1/\sqrt{\epsilon})$  when  $Gr$  is not small. Equation (29), however, indicates that the merit of the heating to stabilize the boundary layer starts to fade away at  $x \sim O(\alpha \Delta T/\epsilon)^{1/2}$  and disappears before the magnitude of the cross flow becomes appreciable, if  $\alpha \Delta T$  is small.

The explicit expression of Eq. (29) in terms of physical quantities can be written as

$$x \sim \sqrt{\frac{\alpha}{a\beta g \cos \phi}} \cdot u_{\infty} \quad (30)$$

Equation (30) reveals that the size of the stabilized region by heating is proportional to the free stream speed, is inversely proportional to the square root of the cylinder diameter, and is independent on  $\Delta T$ . For a cylinder of 1 ft in radius submerged in 60°F water,  $x$  is about 15 at  $u_{\infty} = 3$  ft/sec and 150 at  $u_{\infty} = 30$  ft/sec for  $\phi = \pi$ . This shows that stabilizing the boundary layer by heating a small body is highly effective. However, extrapolating the test data of a smaller body to a larger size appears to be dubious. Furthermore, the existence of the inflection point in the cross-flow velocity could cause earlier separation and shift the transition point upstream.



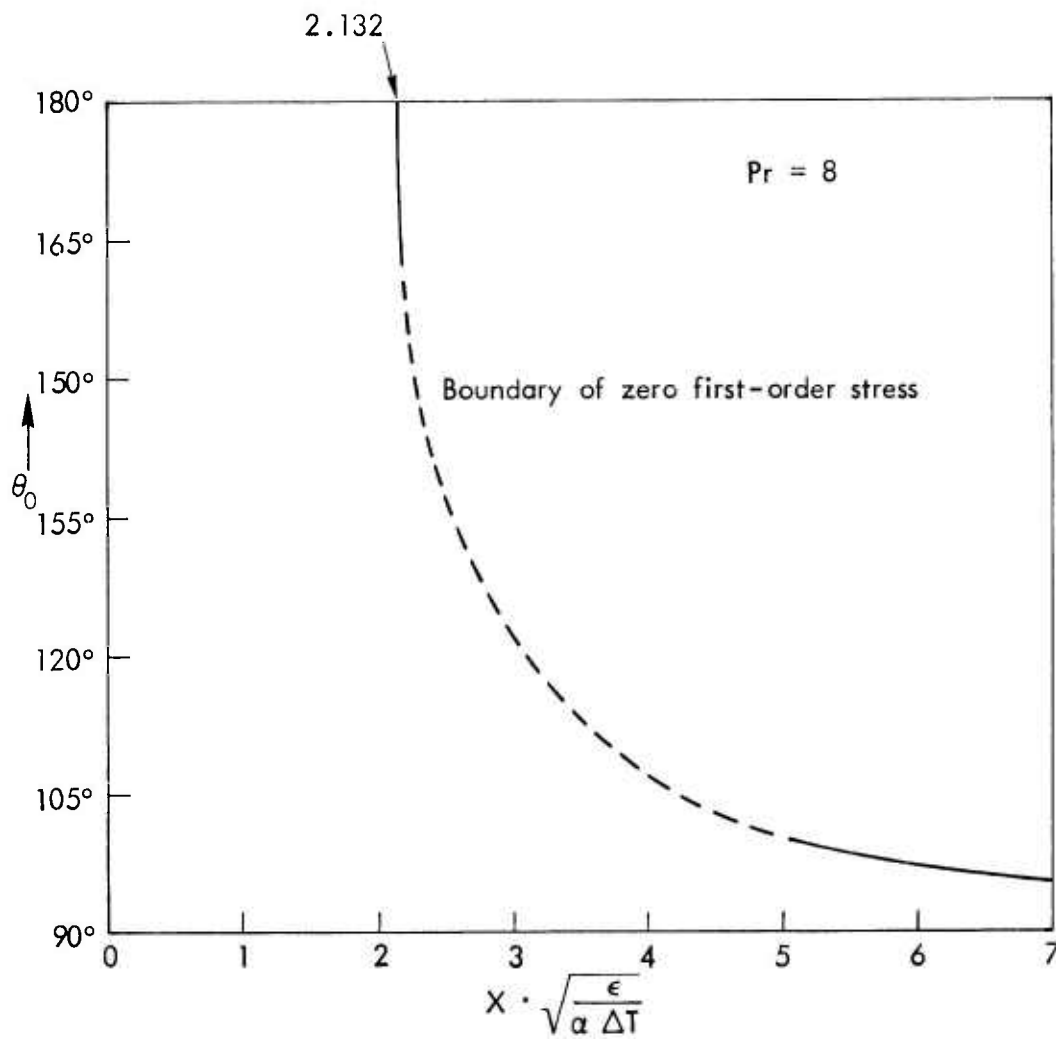


Fig. 7 — Boundary where the variable-viscosity effect balances the cross-flow effect

REFERENCES

1. Schlichting, H., *Boundary Layer Theory*, 6th ed., McGraw-Hill, 1968.
2. Aroesty, J., and S. A. Berger, *Controlling the Separation of Laminar Boundary Layers in Water: Heating and Suction*, The Rand Corporation, R-1789-ARPA, September 1975.
3. Yao, L. S., and I. Catton, *Buoyancy Cross-Flow Effects on the Boundary Layer of a Heated Horizontal Cylinder*, The Rand Corporation, R-1907-ARPA, April 1976.
4. Wazzan, A. R., and C. Gazley, Jr., "A Parametric Study of Boundary-Layer Stability and Transition for Falkner-Skan Wedge Flows," presentation at *Low-Speed Boundary-Layer Transition Workshop: II*, held at The Rand Corporation, Santa Monica, California, September 13-15, 1976.